Ross J. Angel*, Sula Milani, Matteo Alvaro and Fabrizio Nestola

# High-quality structures at high pressure? Insights from inclusions in diamonds

DOI 10.1515/zkri-2016-1949
Received April 4, 2016; accepted June 1, 2016; published online June 28, 2016

**Abstract:** We describe the experimental protocols necessary to measure the crystal structures of minerals trapped within diamonds by single-crystal X-ray diffraction to the same quality as obtained from minerals studied at ambient conditions. The results show that corrections for X-ray absorption in complex cases can be made with good precision. Comparison of the refined structure of a single-crystal olivine inclusion inside a diamond with the structure of a similar olivine held in a high-pressure diamond-anvil cell shows that data resolution, not the correction for absorption effects, is the dominant factor in influencing the quality of structures determined at high pressures by single-crystal X-ray diffraction.

**Keywords:** diamond; diamond-anvil cell; olivine; structure refinement.

## Introduction

To obtain accurate and precise crystal structures by refinement to X-ray diffraction data, it is necessary to have accurate and precise measurements of the intensities of diffracted beams from the sample to high resolution. It has long been recognized that the lower precision and accuracy of crystal structures determined by single crystal diffraction in diamond-anvil pressure cells (DACs), at high pressures, compared to structures determined from crystals in air, is due to a combination of three factors: (i) the restricted access to the reciprocal space of samples, (ii) the absorption by the cell components, and (iii) the structured background in the diffraction patterns that arises from diffraction from the DAC components. Scattering from the cell components used to be dominated by the use of beryllium backing plates (e.g. [1]), but their replacement with diamond backing plates [2] or the use of Boehler–Almax seats [3] which have no backing plates in the X-ray beam have eliminated this problem. The use of finely-collimated or focused X-ray beams at synchrotrons or from laboratory micro-sources greatly reduces the illumination of the gasket, and the only remaining significant contribution to the diffraction pattern in addition to the sample crystal is from the diamonds themselves. However, the relative roles of data access and cell absorption in degrading the quality of high-pressure data have never been completely separated. Restricted datasets have been collected from crystals in air and compared to the results from crystals in DACs, but there has been no way to collect complete full-resolution datasets affected by complex absorption issues. High-quality single-crystal inclusions trapped inside natural diamonds, along with the development of techniques to measure them [4], now provide the opportunity to separate these two issues of absorption correction and data access in high-pressure single-crystal refinements. In this contribution we document the procedures necessary to obtain high-quality X-ray diffraction data from single crystals trapped as inclusions in diamonds, and then use these data to show that the absorption corrections made by modern software are sufficient to allow accurate and precise crystal structures to be determined by refinement. Comparisons with data collected from an olivine crystal held in a DAC then confirm the dominant role of reciprocal space access in determining the quality of high-pressure crystal structures from modern diffraction data.

***Corresponding author: Ross J. Angel,** Department of Geosciences, University of Padua, Via Gradenigo 6, I-35131, Padua, Italy, E-mail: rossjohnangel@gmail.com
**Sula Milani and Fabrizio Nestola:** Department of Geosciences, University of Padua, Via Gradenigo 6, I-35131, Padua, Italy
**Matteo Alvaro:** Department of Earth and Environmental Sciences, University of Pavia, Via A. Ferrata, 1, I-27100 Pavia, Italy

## Experimental

The natural diamond with olivine inclusions discussed in this paper is typical of the suite of diamonds from the Udachnaya kimberlite pipe in Siberia previously studied to determine the relative orientations of the olivines and their diamond host crystals [5]. The diamond is octahedral in form (Figure 1) with edge lengths of ~2.5 mm. It contains several olivine inclusions ranging in size from >200 μm across to <80 μm. For this study we collected an intensity dataset from the inclusion 14A2

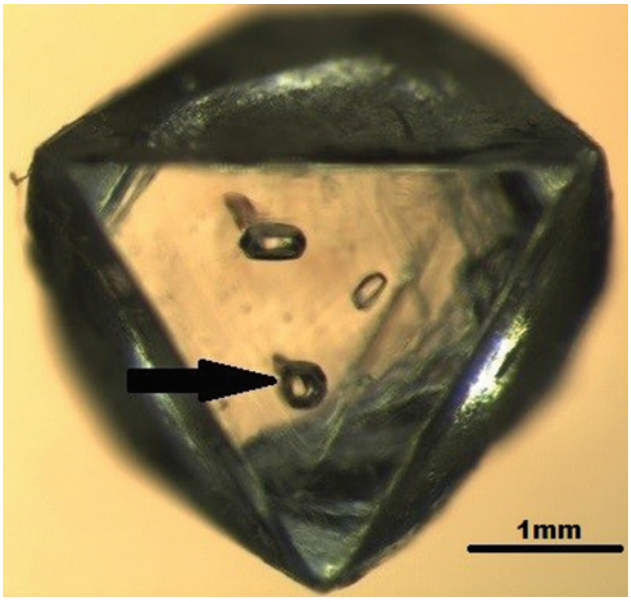


**Fig. 1:** Diamond #14 viewed through an octahedral {111} face. The olivine #14A2 used for this study is indicated by an arrow. Most of the inclusions exhibit {111} faces of the diamond but their random orientations mean that the faces of the olivines are of irrational indices. See reference [5] for further details.

which is approximately equant and ~180 μm in diameter. This olivine inclusion in diamond has an approximate composition as determined by structure refinement of $(Mg_{0.92}Fe_{0.08})_2SiO_4$. The unit-cell parameters of this crystal, as measured in-situ (Table 1), indicate that it is under a residual average stress of ~0.35 GPa, which is typical of olivine inclusions in diamonds (e.g. [4]). Rather than try to match the composition of the inclusion exactly for the DAC measurements, we used a crystal of synthetic end-member forsterite, $Mg_2SiO_4$ [6]. A crystal plate, subparallel to (010), of dimensions $50 \times 85 \times 110$ μm was mounted in a Diacell™ Tozer-type DAC [7] from Almax easy-Lab (www.almax-easylab.com). The cell has Boehler-Almax seats [3] carrying anvils that are 1.45 mm thick. Because the seats are made of tungsten carbide, which is highly absorbing for X-rays, the seats do not diffract X-rays into the detector and therefore make no contribution to the background signal. The DAC measurements were performed at room pressure, without any pressure medium.

All intensity datasets were collected in-house with a Rigaku Oxford Diffraction SuperNova diffractometer equipped with a Mo micro-source X-ray tube and a Dectris Pilatus-200 K detector, controlled by the Crysalis-Pro™ software [8]. With this micro-focus source the full width at half-maximum (FWHM) of the X-ray beam at the sample position is 120–130 μm, so accurate centering of sample crystals on the goniometer is essential for obtaining accurate intensities for high-quality structure refinements. For crystals mounted in air, centering is simply achieved by optical centering using the video microscope. For inclusions in diamonds and crystals in diamond-anvil cells optical access is restricted, and the high refractive index of diamonds leads to large displacements of the image of the crystal, and thus mis-centering of the sample crystal, if it is not viewed through a diamond face perpendicular to the optical axis of the video microscope [9]. For crystals in DACs the DAC is therefore set on the goniometer with the load axis accurately aligned to the X-ray beam when the diffractometer axes are at zero. This ensures that the culet and table faces of the diamond anvils are then perpendicular to the axis of the video microscope when the DAC is moved to the viewing position, and the sample crystal can be accurately centered across the beam. There is no optical access perpendicular to the load-axis of the DAC, so the goniometer head and the microscope focus are adjusted until the crystal remains in optical focus when viewed from both sides of the DAC [9]. Note that this is only possible if both anvils in the DAC have the same thickness, and the microscope has a shallow depth of field.

To perform a similar optical centering procedure for the inclusions inside natural diamonds, the diamond is mounted in wax on a conventional goniometer pin with one external octahedral face of the diamond set perpendicular to the X-ray beam when the diffractometer circles are at zero. This allows the inclusion to be easily viewed in the video microscope through this face, and the inclusion to be centered in directions perpendicular to the beam. Centering of the inclusion along the beam is more difficult because it typically cannot be seen through more than one pair of faces because most diamonds do not display full octahedral morphology. Centering by focusing only works if the inclusion is located exactly in the middle of the diamond, which is not normally the case (Figure 1). We therefore make use of the small FWHM of the beam in the following way. After approximate centering, a rapid intensity data collection is performed with a single $\phi$-scan from 0 to 360°, with a step size of 3–6° per frame, typically in a few minutes. The diffraction pattern is indexed and inspected for the disappearance of diffraction from the sample as it is rotated, which indicates that the inclusion has been moved out of the beam. The diamond is then moved across the beam until indexed diffraction spots from the inclusion are present throughout a 360° $\phi$-scan. Final centering is then performed by integrating the intensities from one of these $\phi$-scans. Frame scale factors are determined as a function of $\phi$ by minimizing the internal agreement factor $R_{int}$ of the intensity data. When a mis-centered inclusion crystal moves out of the center of the beam during rotation on the goniometer, it diffracts less intensity so the frame scale factor becomes larger (Figure 2). If the diamond host crystal was spherical in shape, the frame scale factors should be constant as a function of $\phi$ rotation. Therefore, examination of the pattern of the frame scale factors as a function of $\phi$, and allowing for the influence of absorption of the diamond if it is not equant in shape, allows the position of the inclusion to be deduced, and then adjusted towards the center of the goniometer and the X-ray beam. A couple of iterations of this process of adjustment and 360° $\phi$ intensity data scan are usually sufficient to reduce the range of scale factors to <20% and thus to center the inclusion crystal. Simple geometrical considerations indicate that the precision with which the inclusion can be centered by this method depends on the FWHM of the beam and the size, shape and orientation of the crystal on the goniometer head.

Data collections were set up with the strategy tool in the Crysalis-Pro™ software. For the olivine inclusion we collected intensity data out to $2\theta = 100°$ (resolution 0.46 Å) with an average redundancy of six, so as to enable us to perform accurate frame scaling. The data collection time was 20 h, yielding 2594 frames of data and >10,000 individual intensities. All datasets were integrated within the Crysalis-Pro™ software with a combination of local and global background models to correct for the structured background that arises from scattering from the gasket in the DAC, the tails of the diffraction peaks of the diamonds, and the other inclusions trapped in the same diamond.

**Tab. 1:** Crystallographic parameters from structure refinements to olivine.[a]

| | Inclusion | Inclusion | Inclusion | Crystal in DAC |
|---|---|---|---|---|
| $2\theta_{max}$ | 100° | 70° | 70° | 70° |
| $\Psi_{max}$ | – | – | 35° | 35° |
| Cell parameters | | | | |
| *a* (Å) | 4.7608(3) | | | 4.7561(2) |
| *b* (Å) | 10.1929(8) | | | 10.1989(6) |
| *c* (Å) | 5.9919(4) | | | 5.9812(2) |
| *V* (Å$^3$) | 290.77(4) | | | 290.13(2) |
| Refinement | | | | |
| N reflections | 1625 | 693 | 179 | 174 |
| R1 | 0.017 | 0.012 | 0.012 | 0.014 |
| wR2 | 0.026 | 0.022 | 0.021 | 0.024 |
| Gfit | 0.64 | 0.67 | 0.82 | 0.73 |
| Refined parameters | | | | |
| Mg on M1 | 0.9155(9) | 0.9126(11) | 0.9126(19) | 0.998(3) |
| Mg on M2 | 0.9271(11) | 0.9268(13) | 0.921(3) | 0.997(3) |
| Si–O1 Å | 1.6156(3) | 1.6173(5) | 1.6189(10) | 1.6186(15) |
| Si–O2 Å | 1.6565(4) | 1.6578(5) | 1.656(3) | 1.658(4) |
| Si–O3 Å | 1.6382(3) | 1.6391(4) | 1.6409(11) | 1.6410(14) |
| RMS displacements (Å) | | | | |
| Si → O1 | 0.052 | 0.051 | 0.048 | 0.053 |
| O1 → Si | 0.056 | 0.058 | 0.058 | 0.059 |
| Si → O2 | 0.064 | 0.063 | 0.070 | 0.083 |
| O2 → Si | 0.067 | 0.065 | npd[b] | 0.065 |
| Si → O3 | 0.062 | 0.062 | 0.061 | 0.066 |
| O3 → Si | 0.065 | 0.066 | 0.064 | 0.066 |

[a]The space group of olivine is *Pbnm*.

[b]The refined displacement parameters of O2 were non-positive-definite, so RMS displacements of the O2 oxygen cannot be calculated for this refinement.

Transmission-geometry DACs restrict the maximum 2θ angle at which reflections can be measured to twice the cell opening half-angle $\Psi_{max}$ [1]. Data collection in the DAC was initially performed to collect all accessible data out to $2\theta = 80°$, assuming a cell opening half-angle $\Psi_{max} = 40°$. The effective opening angle of the DAC was then determined by performing a series of integrations of the raw data to different values of $\Psi_{max}$, with $2\theta_{max} = 2\Psi_{max}$. Note that not only are reflections with $\Psi > \Psi_{max}$ excluded from all integration steps, but the corresponding areas of the detector are not used for background evaluation. $R_{int}$ was then calculated for each dataset obtained with each integration. The value of $R_{int}$ is approximately constant for $\Psi_{max} < 35°$, but increases sharply at $\Psi_{max} > 35°$ (Figure 3), which indicates the value of Ψ at which some reflections are partially obscured by the body of the DAC. Final integration of the DAC data was therefore performed with $\Psi_{max} = 35°$ and $2\theta_{max} = 70°$.

For the DAC data, initial absorption corrections to intensity data were made on the basis of the physical dimensions of the diamond anvils and the crystal, using the Absorb-7 program [10] accessed directly from within Crysalis-Pro™. Frame scaling using spherical harmonics was then applied in Crysalis-Pro™ to these corrected data to allow for the effects of small uncertainties in the physical measurements of the DAC and crystal, and for variations in beam illumination of the crystal and for the detector response. For the inclusions, in principle one could build an absorption model of the diamond host crystal as well as the inclusion crystal to make model-based corrections. However, the high optical refractive index of diamond and the rough faces of many diamonds make exact measurements of the sizes of inclusions unreliable. The thickness of the inclusion along the X-ray beam is often particularly difficult to determine. We therefore applied automated frame scaling alone (as implemented in Crysalis-Pro™) to correct for the effects of absorption on the measured diffracted intensities from the inclusion crystals, and we then examined the scale factors for physical reasonableness.

Data from crystals in diamonds and inside diamond-anvil cells can be affected by a number of diffraction events in the diamonds. First, diamond diffraction peaks can overlap or partially overlap the sample peaks on the detector. These sample peaks then have a different shape to the normal diffraction peaks from the sample. Crysalis-Pro™ employs a form of learnt-profile integration, by which these peaks can be identified by their shape parameters and eliminated from the dataset. The diamonds can also reduce the intensity of sample peaks by diffracting away part of the incident beam, or by diffracting the diffracted beam from the sample [11]. These types of events do not change the diffraction profile, but only lower the intensity. We detect and eliminate affected reflections when the symmetry-equivalent reflections are averaged by applying the Blessing criteria for outlier rejection [12] first to the low-intensity outliers, prior to averaging the remaining data in the normal way [13].

Structure refinements were made to the data averaged in Laue group *mmm* with RFINE-2015, a development version of the RFINE-4 program [14], refining to the structure factors *F*. The process of robust-resistant refinement [15] was employed to automatically identify and down-weight any residual outliers that remain in the data. In order to yield correct Mg/Fe site occupancies for the two M

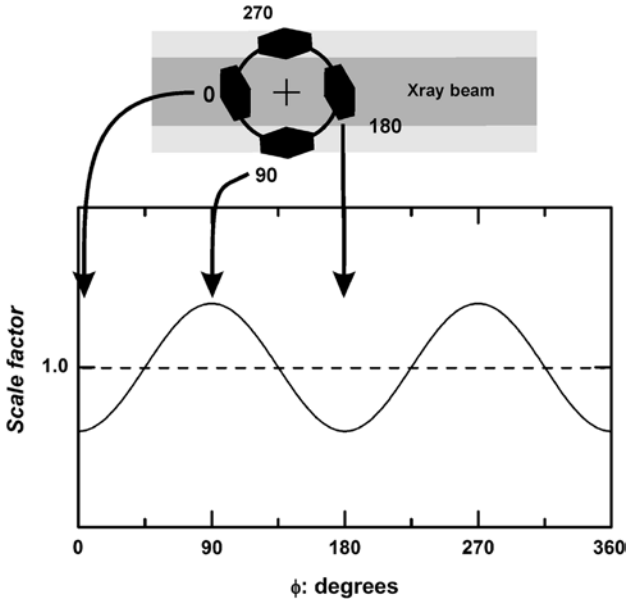


**Fig. 2:** The relationship between frame scale factors and crystal offsets. A plan view of an off-centered crystal (black shape) on the goniometer at $\phi = 0°$, 90°, 180° and 270° is shown at the top. At $\phi = 0°$ and 180° the crystal is completely in the beam, the diffracted intensities are high and thus the scale factors are low. At $\phi = 90°$ and 270° the crystal is only partly in the beam, the diffracted intensities are lower than expected, and so the scale factors are large. Adjustment of the crystal to the goniometer center leads to a smaller scale factor variation, determined only by absorption effects.

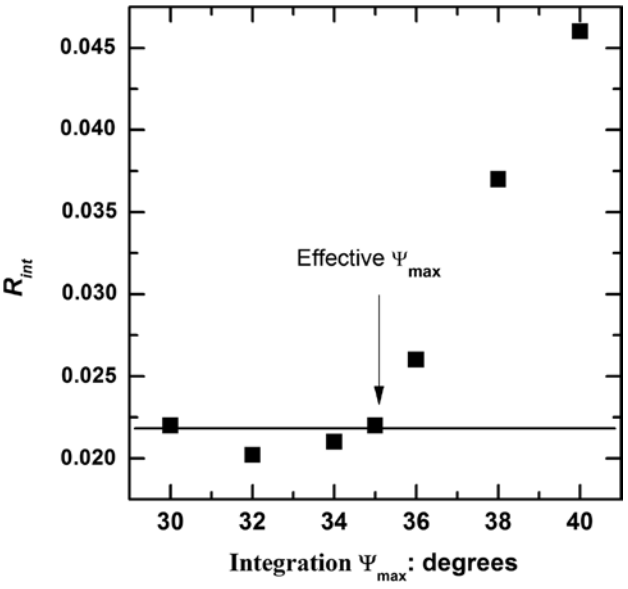


**Fig. 3:** The $R_{int}$ from averaging the intensity data collected in the DAC, as a function of the $\Psi_{max}$ angle used to restrict integration. The rapid increase in $R_{int}$ for $\Psi_{max} > 35°$ indicates that this is the effective opening angle of the DAC.

sites in the olivine structure, the 'electron in bond' model [16, 17] was used. This includes a single electron placed along the Si–O bonds to model the bonding electron density, in combination with fully-ionized scattering factors for the cations, and half-ionized scattering factors for the oxygen atoms. The olivine crystals, even in the diamond, are high quality, so the significant secondary extinction effects were corrected with the Becker-Coppens model [18]. Although the crystal mounted in the DAC was pure $Mg_2SiO_4$, for an exact comparison with the inclusion crystal, the Mg/Fe ratios were still refined for the M sites. These always remained within 1 estimated standard deviation (ESD) of pure Mg, further validating the data quality and the refinement model.

## Results and discussion

As noted above, the X-ray path lengths of each incident and diffracted beam for a single reflection from the olivine inclusion in diamond could in principle be calculated from a physical description of the size and shape of the diamond and the inclusion, and the position of the inclusion within the diamond. However, the variations of absorption corrections expected from the approximately spherical inclusion with an absorption coefficient $\mu_1 = 1.06$ mm$^{-1}$ are small, approximately 2% and are insignificant compared to the absorption variation due to the shape of the diamond. If the inclusion was in the center of the diamond (which it is not), one can estimate the range of scale factors due to absorption by the diamond from the minimum (face–face, ~2 mm) and maximum (vertex–vertex, ~3.5 mm) diameters of the surrounding diamond, as being in the ratio 1:1.3. In our case, the inclusion lies within 300 μm of the nearest diamond face, so one could imagine that the minimum path length for an incident and diffracted X-ray path would be one that enters and exits the nearest diamond surface. This path length would be of the order of 0.8 mm for a Bragg angle of ~45°. Thus the ratio of maximum to minimum frame scale factors due to absorption, $\exp(\mu_{dia}(t_{max} - t_{min}))$, is expected to be less than ~1.7, given that the absorption coefficient for diamond and Mo radiation ($\lambda = 0.7017$ Å) is 0.2 mm$^{-1}$. The actual ratio of maximum to minimum frame scales determined by Crysalis-Pro™ for this dataset was 1.3, which is reasonable considering that it is highly unlikely that the beam paths for a given reflection would enter and exit through apices of the diamond octahedron. After frame-scaling $R_{int} = 0.020$ for averaging 10,418 individual reflection intensities (that were not identified as outliers or space group absences) to 1626 sets of symmetry equivalents. This $R_{int}$ is similar to that achieved from olivine crystals measured in air (e.g. [17]), providing an additional indication that the corrections made by frame-scaling are precise.

The structure refined to the full data set, collected to 100° 2θ (resolution 0.46 Å) and averaged in

the Laue group *mmm*, is reported in the deposited *crystallographic information file* with key results given in the first column of Table 1. Both the statistical measures of fit, and the ESDs on bond lengths and angles are similar to those from olivine crystals measured in air to the same resolution (e.g. [17]). Olivine inclusions in diamonds normally contain trace (<1% total cations) amounts of Mn, Ni and Ca [19]. Therefore, the refined Fe/Mg site occupancies correspond to an effective Mg number of Mg* = (Mg + 0.5*Ca)/(Mg + Fe + Mn + Ni + Ca). Our structure refinements gave Mg* = 0.921(3), which is in the middle of the range of reported compositions for olivine inclusions in diamond [19]. The ESDs on the bond lengths such as Si–O are independent of the direction of the bonds in the crystal structure (Table 1), and the probability displacement ellipsoids look physically reasonable (Figure 4a), with the oxygen ellipsoids slightly elongated perpendicular to their Si–O bonds. Further, the root mean square (RMS) displacements of the Si atom, calculated from the refined anisotropic displacement parameters [20], towards each of the bonded oxygen atoms are ~10% smaller than the corresponding mean displacement of each oxygen towards the silicon (Table 1). This is consistent [21, 22] with the known bonding in olivine, in which the Si–O bonds are strong and the Si–O stretching vibrations are the highest-frequency vibrational modes. The statistical measures of data quality and refinement, together with the quality of the refined structure, indicate that data collected from this inclusion crystal in diamond is of similar quality to that collected from crystals in air. This indicates that frame scaling is capable of successfully correcting intensities for complex absorption cases.

The half-opening angle of the DAC used in this comparison was determined to be 35° (Figure 3), so the DAC data extends only to a maximum 2θ = 70° (resolution 0.62 Å). To provide a fair basis for comparison we therefore cut down the dataset collected from the olivine inclusion to this same resolution and performed a second structure refinement. The refined structural parameters are indistinguishable at the two ESD level from the results of the refinement to the full resolution dataset, but with larger ESDs due to the smaller number of reflections in the dataset (Table 1, and deposited material). Refinement to the DAC data yields the same positional parameters and thus bond lengths, with even larger ESDs due to the smaller number of reflections arising from the restrictions by the body of the DAC. One of the significant differences in the DAC data are in the distribution of these ESDs; the Si–O2 bond length has an ESD of 0.0032 Å, more than twice that of the Si–O1 and O3 bonds of 0.0014 Å. This is because the ESDs in the *y*-coordinates are much larger than those of the *x*- and *z*-coordinates of all of the atoms in the structure. The other significant problem in the DAC refinement is that the displacement ellipsoids are clearly non-physical (Figure 4b), with the RMS displacements of the Si deviating significantly from the displacements of the bonded oxygen atoms (Table 1). This can be traced to the much larger ESDs and disturbed values of the $U_{22}$ component of the displacement tensor of each atom. The reason that both fractional coordinates and tensor components associated with the *b*-axis of the crystal show larger ESDs is because the DAC dataset only contains data with *k* indices up to 5, whereas the dataset from the olivine inclusion restricted to 2θ = 70° has data with *k* = 16. This restriction in the data occurs because the olivine crystal was aligned so that its *b*-axis was 14° from the load axis of the DAC. Exactly the same pattern of larger ESDs and problems with $U_{22}$ displacement parameters is also found in a refinement to the inclusion data further restricted to those reflections only accessible in the DAC (Figure 4c, Table 1 and deposited material). In

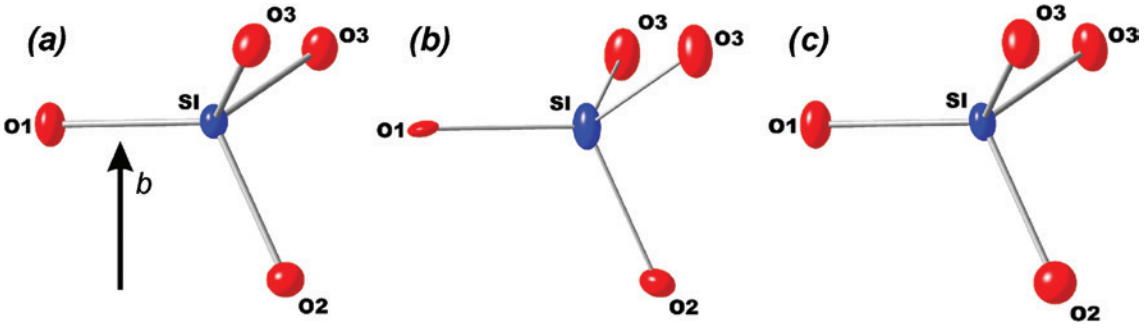


**Fig. 4:** Probability ellipsoids of the $SiO_4$ group drawn at 90% level. (a) Refinement to the inclusion full dataset. The plot for the dataset restricted to 2θ = 70° looks identical. (b) Refinement to the DAC data has the ellipsoid of O1 flattened along [010] and the other atoms elongated in this direction. (c) Refinement to the inclusion data restricted to the same reflections accessible in the DAC shows the similar problems to (b). The O2 atom displacement parameters refined to non-positive-definite values, so it is shown as a sphere in (c).

both cases, the values of parameters such as $U_{22}$ differ from the full refinement by <1 combined ESD, but these ESDs are sufficiently large to include shifts in $U_{22}$ that make the resulting structural model of atomic displacements non-physical.

## Conclusions

The high quality of the crystal structure refinements to data collected from the olivine trapped as an inclusion inside a diamond, as measured by the small ESDs on bond lengths and small *R*-values, and indicated by the physically-meaningful site occupancies and atomic displacement parameters, demonstrates that complex absorption corrections can be made accurately with modern software provided that the original intensity data are precise and of sufficient coverage and redundancy. Comparison to the structure refinement to data collected from a crystal in a DAC therefore confirms that the quality of high-pressure structures is primarily limited by the restricted reciprocal space access provided by transmission-type DACs, and is not due to limitations in the corrections for DAC absorption or to failure to identify other artifacts in the data. These limitations could be overcome by collecting data from several sample crystals mounted together in different orientations in one DAC, and subsequently merging the data prior to refinement. If the multiple crystal samples can be simultaneously illuminated by the incident X-ray beam, then there is the opportunity to apply a single frame-scaling correction to the combined intensity data sets, thereby over-coming the uncertainties in the frame scales when only relative sparse data is available from one crystal.

**Acknowledgments:** This work was supported by ERC grant 307322 which funds the INDIMEDEA project to Fabrizio Nestola. We thank Koen De Hantsetters of Almax easyLab (www.almax-easylab.com) for loaning the Diacell™ Tozer DAC to us for these measurements and for loading the cell. We thank Jeff Harris (Glasgow) for the loan of the diamond used in this study and Katharine Marquardt (Bayreuth) for the synthetic forsterite crystal for the DAC data collection. Javier Gonzalez-Platas (Tenerife), Ronald Miletich (Vienna), Paolo Nimis (Padova), Bernd Maier (Munich) and Mathias Meyer (Rigaku Oxford Diffraction) are thanked for advice and discussions, and two anonymous reviewers provided valuable suggestions for improving the manuscript.

## References

[1] R. J. Angel, R. T. Downs, L. W. Finger, High-temperature and high-pressure diffractometry. in *High-Temperature and High-Pressure Crystal Chemistry*, (Eds. R. M. Hazen and R. T. Downs) Reviews in Mineralogy and Geochemistry, Vol. 41, Mineralogical Society of America and Geochemical Society, Washington, DC, p. 559, **2000**.

[2] B. Periotto, F. Nestola, T. Balic-Zunic, R. J. Angel, R. Miletich, L. A. Olsen, Comparison between beryllium and diamond backing plates diamond anvil cells: application to single-crystal X-ray diffraction high-pressure data. *Rev. Sci. Inst.* **2011**, 055111.

[3] R. Boehler, K. De Hantsetters, New anvil design in diamond-cells. *High-Press. Res.* **2004**, *24*, 391.

[4] F. Nestola, P. Nimis, L. Ziberna, M. Longo, A. Marzoli, J. W. Harris, M. H. Manghnani, Y. Fedortchouk, First crystal-structure determination of olivine in diamond: composition and implications for provenance in the Earth's mantle. *Earth Planet. Sci. Letts.* **2011**, *305*, 249.

[5] F. Nestola, P. Nimis, R. J. Angel, S. Milani, M. Bruno, M. Prencipe, J. W. Harris, Olivine with diamond-imposed morphology included in diamond. Syngenesis or protogenesis? *Inter. Geo. Rev.* **2014**, *56*, 1658.

[6] S. Heinemann, R. Wirth, M. Gottschalk, G. Dresen, Synthetic [100] tilt grain boundaries in forsterite: 9.9 to 21.5°. *Phys. Chem. Minerals* **2005**, *32*, 229.

[7] D. Graf, R. Stillwell, K. Purcell, S. Tozer, Nonmetallic gasket and miniature plastic turnbuckle diamond anvil cell for pulsed magnetic field studies at cryogenic temperatures. *High-Press. Res.* **2011**, *31*, 533.

[8] Rigaku Oxford Diffraction, *Crysalis-Pro software system, version 1.171.38.41, Rigaku Corporation*, Oxford, UK, **2016**.

[9] R. Miletich, D. R. Allan, W. F. Kuhs, High-pressure single-crystal techniques. in *High-Temperature and High-Pressure Crystal Chemistry*, (Eds. R. M. Hazen, and R. T. Downs), Reviews in Mineralogy and Geochemistry, Vol. 41, Mineralogical Society of America and Geochemical Society, Washington, DC, p. 445, **2000**.

[10] R. J. Angel, J. Gonzalez-Platas, Absorb7 and Absorb-GUI for single-crystal absorption corrections. *J. Appl. Crystallogr.* **2013**, *46*, 252.

[11] J. S. Loveday, M. I. McMahon, R. J. Nelmes, The effect of diffraction by the diamonds of a diamond-anvil cell on single-crystal sample intensities. *J. Appl. Crystallogr.* **1990**, *23*, 392.

[12] R. Blessing, Data reduction and error analysis for accurate single crystal diffraction intensities. *Crystallogr. Rev.* **1987**, *1*, 3.

[13] R. J. Angel, *Average*. www.rossangel.net, **2004**.

[14] L. Finger, E. Prince, *A system of Fortran-IV computer programs for crystal structure computations. NBS Technical Note 854*. National Bureau of Standards, Gaithersburg, MD, USA, **1974**.

[15] E. Prince, D. M. Collins, Refinement of structural parameters, 8.2: Other refinement methods. in *International Tables for X-ray Crystallography C*, (Ed. E. Prince) International Union of Crystallography, Kluwer Academic Publishers, Dordrecht, 2005.

[16] R. Heinemann, V. Staack, A. Fischer, H. Kroll, T. Vad, A. Kirfel, Temperature dependence of Fe, Mg partitioning in Acapulco olivine. *Amer. Mineral.* **1989**, *84,* 1400.
[17] R. J. Angel, F. Nestola, A century of mineral structures: how well do we know them? *Amer. Mineral.* **2016**, *101*, 1036.
[18] P. Becker, P. Coppens, Extinction within the limit of validity of the Darwin transfer equations. I. General formalisms for primary and secondary extinction and their application to spherical crystals. *Acta Crystallogr. A* **1974**, *30*, 129.
[19] T. Stachel, J. W. Harris, The origin of cratonic diamonds – constraints from mineral inclusions. *Ore Geol. Revs.* **2008**, *34,* 5.
[20] K. N. Trueblood, H.-B. Bürgi, H. Burzlaff, J. D. Dunitz, C. M. Gramaccioli, H. H. Schulz, U. Schuemli, S. C. Abrahams, Atomic displacement parameter nomenclature. *Acta Crystallogr. A* **1996**, *52*, 770.
[21] M. Kunz, T. Armbruster, Difference displacement parameters in alkali feldspars: effects of (Si, Al) order-disorder. *Amer. Mineral.* **1990**, *75*, 141.
[22] R. T. Downs, G. V. Gibbs, M. B. Boisen, A study of the mean-square displacement amplitudes of Si, Al and O atoms in framework structures: evidence for rigid bonds, order, twinning and stacking faults. *Amer. Mineral.* **1990**, *75*, 1253.